ORIGINAL SCIENTIFIC ARTICLES

Effect of Same-dose Single or Dual Field Irradiation on Damage to Miniature Pig Parotid Glands

Xing Yan[1,2], Bo Hai[2], Zhao-chen Shan[1], Chang-yu Zheng[3], Chun-mei Zhang[1], Song-lin Wang[1,4]*

[1]Salivary Gland Disease Center and the Molecular Laboratory for Gene Therapy, Capital Medical University School of Stomatology, Beijing, China

[2]Beijing Friendship Hospital, Capital Medical University, Beijing, China

[3]Gene Therapy and Therapeutics Branch, National Institute of Dental and Craniofacial Research, NIH, DHHS, Bethesda, MD, USA

[4]Department of Biochemistry and Molecular Biology, Capital Medical University, Beijing, China

Abstract

Xing Yan, Bo Hai, Zhao-chen Shan, Chang-yu Zheng, Chun-mei Zhang, Song-lin Wang. Effect of Same-dose Single or Dual Field Irradiation on Damage to Miniature Pig Parotid Glands. *International Journal of Oral Science*, 1(1): 16–25, 2009

Aim To evaluate the effect of single or dual field irradiation (IR) with the same dose on damage to miniature pig parotid glands.

Methodology Sixteen miniature pigs were divided into two IR groups (n=6) and a control group (n=4). The irradiation groups were subjected to 20 Gy X-radiation to one parotid gland using single-field or dual-field modality by linear accelerator. The dose-volume distributions between two IR groups were compared. Saliva from parotid glands and blood were collected at 0, 4, 8 and 16 weeks after irradiation. Parotid glands were removed at 16 weeks to evaluate tissue morphology.

Results The irradiation dose volume distributions were significantly different between single and dual field irradiation groups (t=4.177, P=0.002), although dose volume histogramin (DVH) indicated the equal maximal dose in parotid glands. Saliva flow rates from IR side decreased dramatically at all time points in IR groups, especially in dual field irradiation group. The radiation caused changes of white blood cell count in blood, lactate dehydrogenase and amylase in serum, calcium, potassium and amylase in saliva. Morphologically, more severe radiation damage was found in irradiated parotid glands from dual field irradiation group than that from single field irradiation group.

Conclusion Data from this large animal model demonstrated that the radiation damage from the dual field irradiation was more severe than that of the single field irradiation at the same dose, suggesting that dose-volume distribution is an important factor in evaluation of the radiobiology of parotid glands.

Keywords irradiation damage, miniature pig, parotid gland

Document code: A **CLC number:** R781.7 Received Sep.9,2008; Revision accepted Nov.24, 2008

Introduction

Radiotherapy for patients with head and neck malignancies often results in long-term irreversible damage to salivary glands in the radiation field (Harrison *et al.*, 2003; Perez *et al.*, 2004), leading to distressing oral complaints, such as xerostomia (Jensen *et al.*, 2003; Vissink *et al.*, 2003). The remarkable radiosensitivity of the parotid gland compared with the submandibular or sublingual glands has puzzled researchers in the field of radiation oncology. At this date, mechanisms of radiation-induced damage in the parotid gland are not fully understood.

The maximum dose and volume of irradiation delivered to targeted tissue are two major factors which are most relevant to the degree of radiation damage. In clinical radiotherapy, the maximum dose can be generally limited by the tolerance dose of healthy normal tissues. Reducing the irradiated volume is more complicated than dose-limiting because of the topographical heterogeneity in tissues such as the parotid gland (Hopewell *et al.*, 2000). In the literature, a single-field irradiation (IR) with different dosages of 15 or 30 Gy was used to investigate IR damage to parotid glands in most studies, yet little is known about effect of single or dual field IR with the same dose on the parotid glands (Li *et al.*, 2005; Nagler, 2001; Friedrich *et al.*, 2002). Currently, several new radiation methods, such as three-dimensional conformal radiation therapy (Malouf *et al.*, 2003) and intensity-modulation radiated therapy (Hondt *et al.*, 1998; Münter *et al.*, 2002) and multi-field IR, are used in clinical radiotherapy (Parliament *et al.*, 2004). Therefore, it is important to understand the relationship between radiation damage and dose-volume distribution in parotid glands induced by different IR fields.

Most previous studies related with IR effects on salivary gland function used rodents as models (Nagler, 2001; Friedrich *et al.*, 2002). The rodent salivary glands, however, have a different radiosensitivity and anatomical structure from human glands (Nagler, 2003). Miniature pig parotid glands do share several anatomic and physiologic characteristics with human glands although they are not identical to human parotid glands (Lotz *et al.*, 1990; Wang *et al.*, 2007). Miniature pigs are also a relatively suitable large animal experimental model with a similar proportional weight to humans, and have been suggested as an appropriate model for the study of functional and histological damages resulting from IR (Radfar and Sirois, 2003). We investigated morphologically, biochemically and physiologically radiation damage to miniature pig parotid glands with an IR megadose at different dose-volume distributions resulting from single- or dual-field IR.

Methods and materials

Animals

Sixteen healthy, male miniature pigs, weighting 30–40 kg and 6–8 months old, were obtained from the Institute of Animal Science of the China Agricultural University. Animals were housed in stainless-steel cages (one pig/cage) with free access to water and food. All animals were acclimatized for at least 2 weeks before the study began. All experiments were reviewed and approved by the Animal Care and Use Committees of Capital Medical University, China.

Parotid gland irradiation

Animals were randomly divided into three groups. Two groups (n=6 each) were irradiated, and the other (n=4) served as control. Before all experimental procedures, miniature pigs were anesthetized with an intramuscular injection of a combination of ketamine chloride (6 mg/kg) and xylazine (0.6 mg/kg). Initially, selecting a single parotid gland on one side of each animal, we administered 4 mL of 40% iodinated oil (Shanghai SinYi Medical, China) as contrast medium intraorally via Stensen's duct. We then performed computerized tomographic scans in the axial cut to determine the IR plan using a 3-D treatment planning system (TPS) (Pinnacle^3, version 7.6, ADAC Inc., USA). The parotid gland on the targeted side was assumed to be the target volume, and the nearby organs were identified as experiencing limited exposure. The isocenter is usually defined as being where the bodys midline crosses at the level of the eyes; for this study, the reference point for all dose calculations was the center of the parotid gland. The maximal dose was 20 Gy for the two groups. For the first group, we used single-field technology with a gantry angle (GA) of zero degrees. We used dual-field technology in the second group, with GA=0° and GA=180° for the two fields, respectively. The radiation field size (non-symmetry field structure) for each group was the same at 12 cm×10 cm. Animals were irradiated with a Varian linear accelerator (Clinac 600C, VARIAN Medical Systems Inc., USA) with 6 MV photon energy at 3.2 Gy/min. The calculated (alpha/beta; about 8.0, an assumption for oral soft tissue) biologic effective dose of a single-time irradiation was equal to a conventional fractionation of 56 Gy in 28 fractions of 2 Gy/d. The control group of miniature pigs were anesthetized

at the same time, but received no IR.

Saliva collection

All saliva collections were done within a specific time period (9 A.M. to 11 A.M.), immediately before IR, then at 4, 8, and 16 weeks after IR. Anesthetized animals were placed on their backs on a "V"-shaped shelf. Modified Lashley cups were placed over the orifice of the parotid ducts bilaterally. Pilocarpine was used to stimulate salivary flow (0.1 mg/kg, intramuscular injection). The first drop of saliva was discarded, and the collection was timed for a total of 10 minutes. Salivary flow rates were expressed as microliters per 10 minutes per gland.

Clinical laboratory analyses

Blood was collected from all animals' vena cava at the same time points as the saliva collection. Serum was separated by centrifugation of the blood samples at 5000 r/min for 2 minutes at room temperature. Blood and saliva were analyzed by standard clinical procedures. Saliva chemistries included measurements of calcium, potassium, sodium, chloride and amylase levels. Serum chemistries included calcium, potassium, sodium, chloride, phosphoreum, glucose, total protein, globulin, aspartate aminotransferase, alanine aminotransferase, lactate dehydrogenase, blood urea nitrogen, alkaline phosphatase, amylase and creatinine. Hematology included the number of white blood cells, red blood cells, concentration of hemoglobin and a primed lymphocyte test.

Tissue preparation and histological evaluation

At 16 weeks the parotid glands from all three groups were harvested carefully. Tissues were fixed by immersion in 10% formalin, and embedded in paraffin, and sectioned at 3–4 μm. Sections were stained with hematoxylin and eosin and examined. Sections, selected randomly from irradiated glands and control glands, were analyzed by a quantitative histopathologic assessment. At 40 times magnification, in 10 successive fields of each section, the area of all recognizable acini was measured using image analysis software (Color Medicine Image Analyzing System, Motic, China). The histopathologic examination was independently performed by a pathologist, blinded to the experimental design and treatment.

Statistical analysis

Data shown are mean values ± SD ($\bar{\chi} \pm s$). All data were analyzed using two-way ANOVA plus Student-Newman-Keuls test or *t*-test with SPSS software (version 11.5).

Results

Irradiation dose distribution in parotid glands

The maximum IR dose for the two IR groups was identical. However, the mean dose and standard deviation of dose distribution between the two IR groups were significantly different (Table 1). The dose–volume histogram demonstrated a more equal dose distribution was found in the dual-field IR group than that in the single-field IR group (Figure 1).

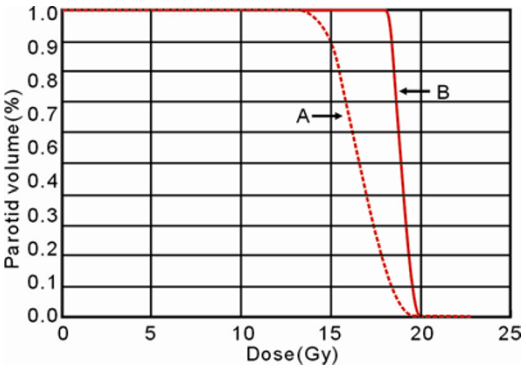

Figure 1 Dose-volume histogram (DVH) of miniature pigs

(A): The DVH of the parotid in single-field irradiation of miniature pigs. (B): The DVH of the parotid in dual-field irradiation of miniature pigs.

Parotid gland morphology and weights

Four weeks after receiving 20 Gy, the parotid glands of the two irradiated groups exhibited engorgement, which was more severe in the dual-fields group. In this latter group, along with the slowly increasing engorgement, we observed ulceration and encrusting of adjacent tissues. The tissue

Table 1 Dose-volume histogram of miniature pigs

	IR dose distribution in the parotid (cGy)			
IR Side	Min	Max	Mean	Std. Dev.
Single field	1292.5	2001.4	1657.2*	131.6
Dual field	1387.8	2001.1	1892.0	40.5

*Significant difference in the mean of irradiation (IR) dose distribution between the single- and dual-field groups (t=4.177, P=0.002).

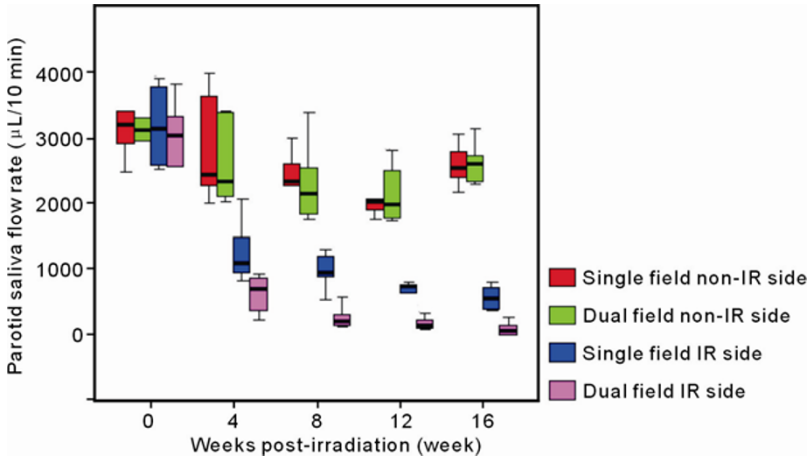

Figure 2 Parotid saliva flow rate after irradiation

The parotid saliva flow rates of targeted glands in both single- and dual-field groups decreased significantly. The decrease in saliva output was more pronounced in the dual-field group. The changes in saliva output from non-IR glands were negligible. Parotid saliva flow rate with 95% confidence intervals (CIs) is shown in a box plot. The upper boundary of the box represents the 75th percentile of the saliva flow per side parotid per 10 minutes. The lower boundary of the box represents the 25th percentile of the data distribution. The horizontal line within the box represents the median value, and the error bars represent the 95% CIs. The closed circles above and below the bars represent out-of-range values.

sloughed at 12 weeks after IR in this group, exhibiting remarkable atrophy and partial depression. Parotid glands in the single-field group did not present these subsequent morphologic changes.

There were significant decreases in the gross weight of IR-side parotid glands at 16 weeks after exposure. For 20 Gy of single-field IR, gland weights decreased from (35.2±2.1) g/gland to (16.5±2.0) g/gland (t=14.214, P=0.000); with 20 Gy of dual-field IR, however, an even greater decrease in gland weights occurred, to (9.3±1.8) g/gland (t=20.920, P=0.000). No changes in gland weights were seen at the 16-week time point after IR in the contralateral gland (single-field: (34.8±1.9) g/gland; dual field: (35.6±2.5) g/gland after 16 weeks). There were significant differences in treated gland weights between the single-field and dual-field groups at 16 weeks post-IR (t=6.554, P=0.000).

Effect of irradiation on miniature pig parotid flow rates

The quantity of saliva in irradiated parotid glands showed that in the single-field group, saliva flow rates on irradiated sides had decreased 61%, 70%, 79%, and 82% at 4, 8, 12, and 16 weeks post-IR (P<0.001, two-way ANOVA), but the non-irradiated sides exhibited smaller changes: 14%, 28%, 35%, and 34% reduction in saliva production at the same time points, respectively (Table 2, Figure 2). The saliva flow rates on the irradiated sides in the dual-field group had decreased 79%, 92%, 95%, and 98% at 4, 8, 12, and 16 weeks post-irradiation (P<0.001); the nonirradiated sides showed a 17%, 27%, 32%, and 26% reduction in saliva production at the same respective time points. In a comparison of the single-field and dual-field groups, parotid flow rate decrease on the irradiated

sides was significantly different at 4 weeks (t= 2.825, P=0.018), 8 weeks (t=5.588, P=0.000), 12 weeks (t=6.742, P= 0.000), and 16 weeks (t=5.841, P=0.001) post-IR, while the flow rates on the non-irradiated sides showed no significant difference.

Clinical laboratory changes

As shown in Table 3, after 20 Gy IR to the parotid gland on one side, several transient alterations were detected in serum hematology and chemistry parameters. The significant differences were seen for WBCs (white blood cells) and amylase at 4 weeks post-IR. However, the variation gradually diminished. We found no significant differences between values before IR and those at 16 weeks post-IR. Essentially, all other changes in serum chemistry and hematology parameters were within normal limits (e.g., lactate dehydrogenase, platelets; summarized in Table 3).

As shown in Table 4, there were several significant alterations in salivary chemistry parameters

Table 2 Parotid saliva flow rate in same-dose single or dual field irradiation

	Single field (20 Gy)		Dual fields (20 Gy)	
	Non-IR side	IR side	Non-IR side	IR side
Pre-IR	3236±613	3164±625	3117±526	3043±502
IR+4 weeks	2779±810*	1242±454*	2584±625*	625±283*#
IR+8 weeks	2337±468*	959±263*	2288±599*	247±168*#
IR+12 weeks	2095±378*	667±160*	2116±439*	159±92*#
IR+16 weeks	2568±317	557±170*	2605±306	83±103*#

Data are mean values ± SD [$\bar{\chi} \pm s$, μL/(10 min·gland)]. In the single-field group, saliva flow rates on irradiated sides had decreased 61%, 70%, 79%, and 82% at 4, 8, 12, and 16 weeks post-IR (P<0.001, two-way ANOVA), but the non-irradiated sides exhibited smaller changes: 14%, 28%, 35%, and 34% reduction in saliva production at the same time points, respectively. The saliva flow rates on the irradiated sides in the dual-field group had decreased 79%, 92%, 95%, and 98% at 4, 8, 12, and 16 weeks post-irradiation (P<0.001); the non-irradiated sides showed a 17%, 27%, 32%, and 26% reduction in saliva production at the same respective time points. In a comparison of the single-field and dual-field groups, parotid flow rate decrease on the irradiated sides was significantly different at 4 weeks (t=2.825, P=0.018), 8 weeks (t=5.588, P=0.000), 12 weeks (t=6.742, P=0.000), and 16 weeks (t=5.841, P=0.001) post-irradiation, while the flow rates on the non-irradiated sides showed no significant difference.

*significant difference compared with pre-IR (P<0.05).

#significant difference between single- and dual-field groups (P<0.05).

Table 3 Serum hematology values

Parameter	Animals	Unit	Pre-IR	IR-4W	IR-8W	IR-12W	IR-16W
WBC	Single field	$\times10^9$/L	10.12±1.99	5.85±1.21*	5.85±1.21*	9.66±1.17	10.38±1.62
	Dual field	$\times10^9$/L	10.63±1.46	4.90±1.31*	4.90±1.31*	10.32±1.32	9.67±1.58
RBC	Single field	$\times10^{12}$/L	6.13±0.66	6.57±0.77	6.57±0.77	6.55±0.55	6.63±0.67
	Dual field	$\times10^{12}$/L	6.35±0.48	6.70±0.44	6.70±0.44	6.32±0.58	6.47±0.65
PLT	Single field	$\times10^9$/L	311.5±52.9	383.8±78.2	383.8±78.2	363.2±59.6	344.1±117.4
	Dual field	$\times10^9$/L	327.5±74.9	423.3±92.2	423.3±92.2	395.3±73.2	350.2±64.2
LDH	Single field	IU/L	560±88	449±62*	449±62*	557±90	572±81
	Dual field	IU/L	547±104	422±115*	422±115*	594±104	602±92
AMY	Single field	IU/L	1690±304	2193±294*	2193±294*	1992±302	1856±308
	Dual field	IU/L	1641±231	2312±308*	2312±308*	1924±294	1777±275

Data are mean values ± SD ($\bar{\chi} \pm s$) for 6 miniature pigs. The data shown are for parameters that exhibited a significantly different change at 4 and 8 weeks post-irradiation in single- and dual-field irradiation groups (P<0.05). WBCs, white blood cells; AMY, amylase; LDH, lactate dehydrogenase; and PLT, platelet.

*significant difference compared with pre-IR (P<0.05).

Table 4 Salivary chemistry values

Item	Animals	Unit	Pre-IR	IR-4W	IR-8W	IR-12W	IR-16W
Ca^{2+}	Single field	mmol/L	2.94±0.37	1.79±0.39*	1.70±0.42*	1.62±0.38*	1.65±0.34*
	Dual field	mmol/L	2.96±0.41	1.65±0.33*	1.61±0.38*	1.52±0.36*	1.47±0.34*
K^+	Single field	mmol/L	22.2±3.1	29.2±4.0	35.9±5.4*	40.9±7.4*	43.6±7.3*
	Dual field	mmol/L	21.8±3.6	28.3±4.4	37.4±6.7*	43.2±5.8*	46.8±3.3*
AMY	Single field	IU/L	1310±266	1703±381*	1331±238	1090±246	834±263*
	Dual field	IU/L	1293±274	1721±425*	1403±259	1055±275	717±135*

The data shown are mean values ± SD ($\bar{\chi} \pm s$) for 6 miniature pigs. The data shown were significantly changed parameters for Ca^{2+}, K^+, and amylase (AMY) (P=0.000). Two-way ANOVA and Student-Newman-Keuls test were used.

*significant difference compared with pre-IR (P<0.05).

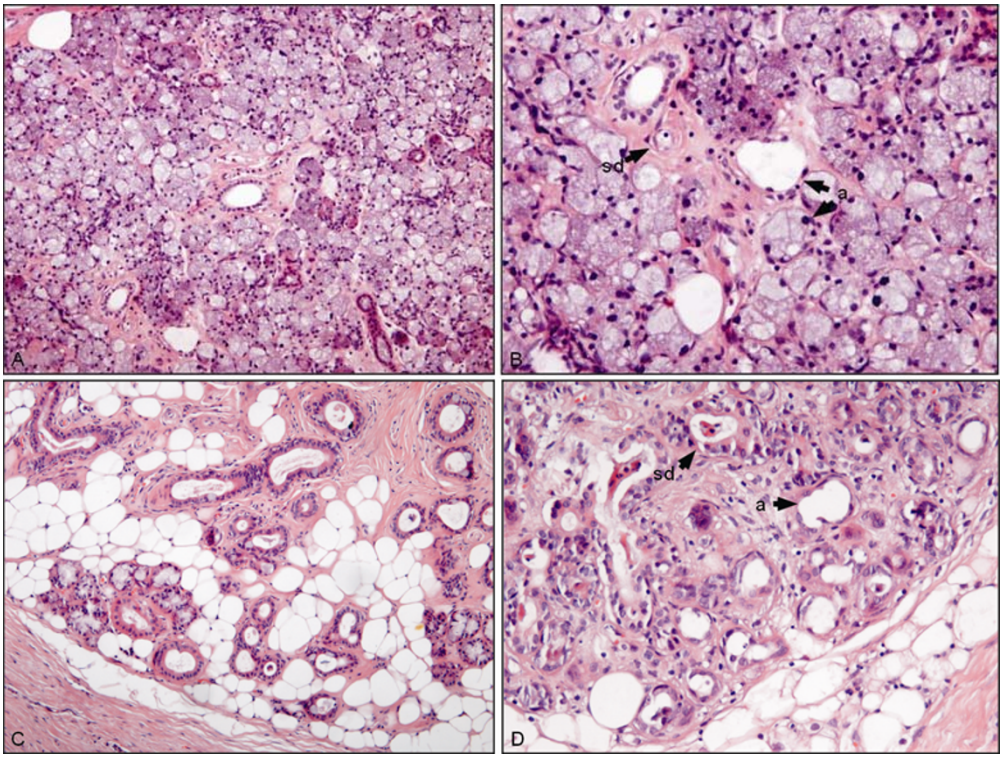

Figure 3 Photomicrographs of parotid gland tissue 16 weeks after 20 Gy IR

(A): Single field IR group (HE, ×100). The lobular structure is generally present. The loss of parenchymal cells and proliferation of interlobular interstitial fibrosis with destruction of lobular architecture is evident. (B): Single-field group (HE, ×200). The acinar structure was not distinct, and exhibited atrophy, degeneration, and partial vacuolization. The vacuolated cytoplasm was present in most acini (a). Destruction of the striated duct (sd) structure with cellular necrosis. A number of ducts were dilated, containing cellular debris and thickened secretions. (C): Dual-field IR group (HE, ×100). The lobular structure was almost completely destroyed with the loss of parenchymal cells, a characteristic lipomatosis, and progressive vacuolization. The acinar cellular frontiers are not present in the majority of the visual field. (D): Dual-field IR group (HE, ×200). The photomicrographs show vacuolization in the overwhelming portion of acinar cells (a). The destruction of acinar architecture, necrosis, and interstitial fibrosis can be seen. The dilated striated duct (sd) system is occluded by fibrous connective tissue.

at 4 weeks post- IR, which were maintained at 16 weeks post-IR, including calcium, potassium, and amylase. At 16 weeks post-IR, salivary calcium levels had decreased significantly in the single-field and dual-field groups. On the other hand, salivary potassium levels at 16 weeks post-IR were significantly higher than pre-IR levels. No significant changes were found in salivarychemistry results from the contralateral glands (data not shown). Salivary amylase secreted from the

targeted glands was significantly increased at 4 weeks; however, they had decreased at 8 weeks, dropping to approxi- mately 60% of pre-IR levels in both IR groups (Table 4).

Histopathologic examination for irradiated parotid glands

Histopathologic examination of parotid gland tissue 16 weeks after IR showed the degradation of the acinar and lobular structures. In the single-field group, the lobular structure predominated, but there was loss of parenchymal cells and proliferation of interlobular interstitial fibrosis with destruction of the lobular architecture (Figure 3). Some acinar structures were indistinct, with atrophy, degeneration, and partial vacuolization. The vacuolated cytoplasm was present in most acini. We also observed destruction of the striated duct structure with cellular necrosis, and a number of ducts exhibited dilation, containing cellular debris and thickened secretions. In the dual-field group, the lobular structure had been severely damaged with the loss of parenchymal cells, a characteristic lipomatosis, and progressive vacuolization. The acinar cellular boundaries were not observed in the majority of the visual field. There were vacuolizations in most of the acinar cells. The destruction of acinar architecture, necrosis, and interstitial fibrosis could be seen. Fibrous connective tissue occluded the dilated duct system.

Discussion

To our knowledge, there are no reports in the literature regarding IR dose distribution with different IR fields in parotid glands in a large animal model. Our study demonstrates a significant difference in IR dose in the parotid between single and dual fields. Use of the dual field presented the more equalized dose distribution; the maximal IR doses in each of the two groups were similar, but the mean values ± SD differed remarkably. The most important factors for the non-homogeneous distribution of IR are the attenuation of the quantity of radiant energy in the tissue, especially in a large target tissue. The parotid is the largest in the salivary glands and is located in the space between the outer ear canal and the mandibular ramus, extending to the posterior portion of the mandible. The miniature pig parotid is heterogeneous, which results in the differences observed in the dose-volume histogram (DVH).

The present study indicated a significantly different DVH in these large animal parotid glands after IR using the same maximal IR dose, an outcome that may influence the curative effects of IR. In addition, damage to tissues may also negatively influence these effects. The exact mechanism of radiation-induced salivary gland damage is unclear. However, some influencing factors correlating to IR-induced damage have been detected. The damage to the salivary glands relates to radiotherapeutic treatment modalities, such as IR dose, IR volume, and fractionation schedule (Seifert *et al.*, 1996; Sagowski *et al.*, 2003). The parotid-sparing radiocurable techniques may center on high-dose radiation to the target tissue while minimizing the IR dose to the parotid glands (Eisbruch *et al.*, 1999; Ship *et al.*, 1997). Nevertheless, for target tissue on head and neck, nearly no radiotherapy procedure can avoid delivery to the parotid glands and eliminate chronic radiation damage.

Patients subjected to radiation therapy often present a noticeable salivary flow rate decrease after an IR dose accumulating to 10–15 Gy or at one week post-IR (Franzen *et al.*,1992; Mossman *et al.*, 1981). The stimulated or resting salivary flow rate is an important parameter indicating post-IR changes (Heinze *et al.*, 1983; Makkonen *et al.*, 1987). In our study, saliva flow rate decreased dramatically at 4 weeks after IR, then continued decreasing through 16 weeks post-IR. In the dual-field group, which received 18.5 Gy IR to a 90% irradiated volume, there was almost no saliva flow rate at 16 weeks post-IR. As for the single-field group, the saliva flow rate at 16 weeks post-IR was approximately 20% of pre-IR values.

We observed some important external changes in the parotid glands that probably resulted in this absence of saliva output. Ulcerating, crusting, and atrophying of tissues in the parotid region would result in a zero saliva output. As for saliva flow rates from the contralateral glands, although they exhibited a significant reduction from pre-IR levels to 12 weeks post-IR, there was no diffe-

rence related to the saliva flow rates of irradiated glands between two groups. In previous studies of patients undergoing parotid gland surgery, after removal of one parotid gland, the contralateral gland showed a compensatory hyperfunction (Cunning *et al.*,1998), which was suggested as a functional reserve of salivary glands (Chaushu *et al.*, 2001; Marunick *et al.*, 1993). The present study showed an increase in saliva output from contralateral, non-IR glands at 16 weeks post-IR and no significant difference compared with pre-IR values.

The pathological changes of radiation injuries for salivary glands are progressive edema, vacuolization, and lipomatosis, which lead to a functional loss (Seifert *et al.*, 1996; Marunick *et al.*, 1987). The atrophic acinar cells, dilated and metaplastic duct system and interstitial fibrosis can be considered the result of such damage. We also observed terminal stage damage in these IR-treated glands, features that included destruction of the lobular structure, dilation of the duct system with obstruction, and hyperplasia of the mucous granuloma (Sagowski *et al.*, 2003). We identified all of these pathological changes in one section, especially in the parotid glands lacking any saliva flow rate, corresponding to the decreased gland weight and atrophy of the parotid region.

We found some important associations between saliva output and gland weight or pathological damage at 16 weeks post-IR. The more severe parotid gland damage in the dual-field group was associated with a greater decrease of saliva flow rate compared to the single-field group. The absent saliva output may be considered as a clinically terminal stage of IR damage to the parotid glands, corresponding to the pathological damage; in addition, the skin ulceration and partial atrophy in the parotid region can be considered a clinical observation.

Also potentially applicable to clinical practice is our finding of some significant changes in saliva chemistry parameters from the target parotid. The temporal increase and then final reduction of salivary amylase might be hypothesized as the initial injury response and subsequent reduction of acinar cells (Valdez *et al.*, 1993; Turner and Sugiya, 2002). The salivary calcium level decreased steadily, a finding mainly associated with acinar cells. Nevertheless, the salivary potassium level increased, a finding consistent with the idea that salivary potassium is secreted by ductal cells (Sagowski *et al.*, 2003); salivary ductal cells are more radioresistant than acinar cells, resulting in a higher cell survival rate post-IR. As for hematology, blood cell count could change after partial radiotherapy (Mauch *et al.*,1995, Yang *et al.*, 1995). Our data showed a temporary decrease in white cell count post-IR, followed by a return to normal levels at 12 weeks post-IR. In dual-field IR, the white cell count increased significantly at 8 weeks post-IR, which was assumed to indicate an inflammatory reaction to the ulceration of the parotid region. The serum amylase levels rose steadily post-IR, and necrosis of the acinar cells is one possible explanation for this increase.

Miniature pigs are a suitable large animal experimental model for assessing parotid gland irradiation damage because of their greater similarity to humans compared to rodent models of clinical conditions (Wang *et al.*, 2007; Wang *et al.*, 1998). A previous study found that using a single megadose of IR (20 Gy) protocol with this species provided a valuable animal model of parotid gland IR damage (Li *et al.*, 2005; Wang *et al.*, 2007). Here, we used this model to obtain findings on saliva flow rate, hematology and salivary chemistry, and histopathology induced by same-dose single or dual field irradiation damage to parotid glands.

Conclusion

Different dose-volume distributions resulting from single-field or dual-field approaches using the same dose of radiation led to significant differences in saliva flow rates and histomorphological damage between these two irradiation groups. These findings suggest that dose-volume distribution is an important factor in evaluation of the radiobiology of parotid glands.

Acknowledgements

This study was supported by the National Natural Science Foundation of China (Grant 30430690) and Beijing Major Scientific Program Grants (D09

06007000091).

References

Chaushu G, Dori S, Sela BA, Taicher S, Kronenberg J, Talmi YP (2001). Salivary flow dynamics after parotid surgery: A preliminary report. *Otolaryngol Head Neck Surg*, 124(3): 270– 273.

Cunning DM, Lipke N, Wax MK (1998). Significance of unilateral submandibular gland excision on salivary flow in noncancer patients. *Laryngoscope*, 108(6): 812–815.

Eisbruch A, Haken RKT, Kim HM, Marsh LH, Ship JA (1999). Dose, volume, and function relationships in parotid salivary glands following conformal and intensity-modulated irradiation of head and neck cancer. *Int J Radiat Oncol Biol Phys*, 45(3): 577–587.

Franzen L, Funegard U, Ericson T, Henriksson R (1992) . Parotid gland function during and following radiotherapy of malignancies in the head and neck: A consecutive study of salivary flow and patient discomfort. *Eur J Cancer*, 28(2–3): 457–462.

Friedrich RE, Bartel-Friedrich S, Holzhausen HJ, Lautenschläger C (2002). The effect of external fractionated irradiation on the distribution pattern of extracellular matrix proteins in submandibular salivary glands of the rat. *J Craniomaxillofac Surg*, 30(4): 246–254.

Harrison LB, Sessions RB, Ki Hong W (2003). Head and neck cancer. A multidisciplinary approach. Philadelphia: Lippincott Williams & Wilkins.

Heinze V, Birkhed D, Björn H (1983). Secretion rate and buffer effect of resting and stimulated whole saliva as a function of age and sex. *Swed Dent J*, 7(6): 227–231.

Hondt E, Eisbruch AE, Ship JA (1998). The influence preradiation salivary flow rates and radiation dose on parotid salivary gland dysfunction in patients receiving radiotherapy for head and neck cancers. *Spec Care Dentist*, 18(3): 102–108.

Hopewell JW, Trott KR (2000). Volume effects in radiobiology as applied to radiotherapy. *Radiother Oncol*, 56(3): 283–288.

Jensen SB, Pederson AM, Reibel J, Nauntofte B (2003). Xerostomia and hypofunction of the salivary glands in cancer therapy. *Support Care Cancer*, 11(4): 207–225.

Li J, Shan ZC, Ou GF, Liu XY, Zhang CM, Baum BJ, Wang SL (2005). Structural and functional characteristics of irradiation damage to parotid glands. *Int J Radiat Oncol Biol Phys*, 62(5): 1510–1516.

Lotz S, Caselitz J, Tschakert H, Rehpenning W, Seifert G (1990). Radioprotection of minipig salivary glands by orciprenaline-carbachol. An ultrastructural and semi-quantitative light microscopic study. *Virchows Arch A Pathol Anat Histopathol*, 417(2): 119–128.

Makkonen TA, Nordman E (1987). Estimation of long-term salivary gland damage induced by radiotherapy. *Acta Oncol*, 26(4): 307–312.

Malouf JG, Aragon C, Henson BS, Eisbruch A, Ship JA (2003). Influence of parotid-sparing radiotherapy on xerostomia in head and neck cancer patients. *Cancer Detect Prev*, 27(4): 305– 310.

Marunick MT, Mahmassani O, Klein B, Seyedsadr M (1993). The effect of surgical intervention for head and neck cancer on whole salivary flow: A pilot study. *J Prosthet Dent*, 70(2): 154–157.

Mauch P, Constine L, Greenberger J, Knospe W, Sullivan J, Liesveld JL, *et al.* (1995). Hematopietic stem cell compartment: Acute and late effects of radiation thetapy and chemotherapy. *Int J Radiat Oncol Biol Phys*, 31(5): 1319–1339.

Mossman KL, Shatzman AR, Chencharick JD (1981). Effects of radiotherapy on human parotid saliva. *Radiat Res*, 88(2): 403–412.

Münter MW, Karger CP, Hoffner SG, Hof H, Thilmann C, Rudat V, *et al.* (2004). Evaluation of salivary gland function after treatment of head-and-neck tumors with intensity-modulated radiotherapy by quantitative pertechnetate scintigraphy. *Int J Radiat Oncol Biol Phys*, 58(1): 175–184.

Nagler RM (2003). Effects of head and neck radiotherapy on major salivary glands—animal studies and human implications. *In Vivo*, 17(4): 369–375.

Nagler RM (2001). Extended-term effects of head and neck irradiation in a rodent. *Eur J Cancer*, 37(15): 1938–1945.

Parliament MB, Scrimger RA, Anderson SG, Kurien EC, Thompson HK, Field G.C, *et al.* (2004). Preservation of oral health-related quality of life and salivary flow rates after inverse-planned intensity-modulated radiotherapy (IMRT) for head-and-neck cancer. *Int J Radiat Oncol Biol Phys*, 58(3): 663–673.

Perez CA, Brady LW, Halperin EC, Schmidt URK (2004). *Principles and practice of radiation oncology*. Philadelphia: Lippincott Williams & Wilkins.

Radfar L, Sirois DA (2003). Structural and functional injury in minipig salivary glands following fractionated exposure to 70 Gy of ionizing radiation: An animal model for human radiation-induced salivary gland injury. *Oral Surg Oral Med Oral Pathol Oral*

Radiol Endod, 96(3): 267–274.

Sagowski C, Wenzel S, Metternich FU, Kehrl W (2003). Studies on the radioprotective potency of amifostine on salivary glands of rats during fractioned irradiation: acute and late effects. *Eur Arch Otorhinolaryngol*, 260(1): 42–47.

Sagowski C, Wenzel S, Tesche S, Jenicke L, Jaehne M (2003). Investigation of radiosialadenitis during fractioned irradiation: sialoscintigraphical and histomorphological findings in rats. *Eur Arch Otorhinolaryngol*, 260(9): 513-517.

Seifert G (1996). Strahlen-Sialadenitis. In: Doerr W, Seifert G, Uehlinger E eds. *Spezielle pathologische Anatomie. Oralpathologie I: Pathologie der Speicheldrüsen*. Berlin: Springer, 196–208.

Ship JA, Eisbruch A, Hondt E, Jones RE (1997). Parotid sparing study in head and neck cancer patients receiving bilateral radiation therapy: 1 year results. *J Dent Res*, 76(3): 807–813.

Turner RJ, Sugiya H (2002). Understanding salivary fluid and protein secretion. *Oral Dis*, 8(1): 3–11.

Valdez IH, Atkinson JC, Ship JA, Fox PC (1993). Major salivary gland function in patients with radiation-induced xerostomia: flow rates and sialochemistry. *Int J Radiat Oncol Biol Phys*, 25(1): 41–47.

Vissink A, Jansma J, Spijkervet FKL, Burlage FR, Coppes RP (2003). Oral sequelae of head and neck radiotherapy. *Crit Rev Oral Biol Med*, 14(3): 199–212.

Wang SL, Liu Y, Fang DJ, Shi ST (2007). Miniature Pig: A Useful Large Animal Model for Dental and Orofacial Research. *Oral Diseases*, 13(6): 530–537.

Wang SL, Li J, Zhu XZ, Sun K, Liu XY, Zhang YG (1998). Sialographic characterization of the normal parotid gland of the miniature pig. *Dentomaxillofac Radiol*, 27(3): 178–181.

Yang FE, Vaida F, Ignacio L, Houghton A, Nautiyal J, Halpern H, *et al.* (1995). Analysis of weekly complete blood counts in patients receiving standard fractionated partial body radiation therapy. *Int J Radiat Oncol Biol Phys*, 33(3): 607–617.

*Corresponding author: Song-lin Wang

Address: Salivary Gland Disease Center and the Molecular Laboratory for Gene Therapy & Tooth Regeneration, Capital Medical University School of Stomatology, Tian Tan Xi Li No.4, Beijing 100050, China

Tel & Fax: 86 10 67062012 E-mail: slwang@ccmu.edu.cn